Towards Unified Framework for Trajectory Optimization using General Differential Kinematics and Dynamics

Eiichi Yoshida and Ko Ayusawa

Abstract This paper presents a new framework for trajectory optimization using comprehensive differential kinematics and dynamics theory, and also its applications and perspectives. For a robotic system with large degrees of freedom including humanoid robots, numerical gradient computation is not practical in terms of precision and time. Trajectory optimization is more and more demanded in different fields not only for usual motion planning but also motion imitation, dynamic parameter identification and human motion understanding. The proposed theory is based on the comprehensive motion transformation matrix (CMTM) that allows describing variational relationship in differential kinematics and dynamics including velocity and acceleration based on a simple chain product. This enables analytical gradient computation of various physical quantities such as joint force or torque with respect to trajectory parameters, which is beneficial to various optimization problems. We overview the possible evolution brought by this technique and demonstrate its advantages through examples of efficient optimization of dynamic motions for a redundant robot and a humanoid under severe constraints. Also, we discuss the possibility of its integration in optimal control method.

1 Introduction

Optimization technique is becoming more and more important in many research fields of robotics to plan and control the motion of various robots. Especially, anthropomorphic systems including humanoid robots and digital human models that we have been working on, are attracting interests because of its widespread application areas. Together with a motion planning method where geometric and kinematic path is first planned and then converted into whole-body trajectory by us-

E. Yoshida and K. Ayusawa,
CNRS-AIST JRL (Joint Robotics Laboratory), UMI3218/RL, Tsukuba Central 1, 1-1-1 Umezono, Tsukuba, Ibaraki 305-8560 Japan e-mail: {e.yoshida, k.ayusawa}@aist.go.jp

ing dynamic locomotion pattern generator and inverse kinematics (IK) for a loco-manipulation task [36, 37], our group also tackled whole-body motion optimization problem [18, 38, 30] that was still challenging at that time as it should take into account many mechanical constraints such as joint or torque limit, as well as constraints like dynamic stability and unilateral contacts at the same time for a large number of degrees of freedom (DOFs).

Whole-body motion optimization technique for anthropomorphic systems keeps evolving for various purposes: dynamic multi-contact motions [16, 9, 32, 8], human motion retargeting [29, 35, 23, 1], and dual-arm manipulation of a flexible object with minimum deformation [25] by humanoid robots. The usage of trajectory optimization for anthropomorphic systems is not limited to humanoid robots, but can be exploited for human motion analysis and understanding. Human motion simulation is one of the typical examples. Self-stable dynamic running motion for a human figure has been generated by determining model parameters and actuation input based on efficient optimal control techniques and stability optimization [19]. Musculoskeletal analysis [21, 11] of a digital human model is another typical application. This study models the muscles as massless wires connecting links and computes muscle tensions by minimizing the total energy and biologically modeled muscle activities under dynamic constraints. Real-time visual feedback of muscular activity was also proposed by introducing fast computation [20, 2].

According to recent progress in robotics and increasing requirements for diverse applications, we are facing more and more complex optimization problems including dynamics, system identification, and motion generation and control. For instance, optimization-based motion planning like CHOMP [26] and trajopt [27] allow continuous path refinement to obtain a collision-free path even the initial path is in collision, based on covariant gradient techniques. The cost function can include such indices like path smoothness, obstacle avoidance and other physical quantities such as object orientation depending on the required task. Another illustrative example is the generation of optimal persistent exciting (PE) trajectory for dynamics parameter identification for humanoid robots [4, 12, 3]. The robot needs to move sufficiently each of its links in a dynamic manner for better identification performance, which is called the persistent exciting motion. It is necessary to minimize the condition number of "regressor matrix" computed from the trajectory while satisfying other constraints such as dynamic balance and mechanical limitations. Here also, gradients of several physical quantities should be computed and it will become intractable with numerical differentiation.

In those complex trajectory optimization problems, the cost function and the constraints often involve combined physical quantities. The partial derivative of any physical quantities with respect to the joint coordinates is therefore indispensable when evaluating the cost and constraints represented by the coordinates and their derivatives, as well as forces in both Cartesian and joint space. Previous work [24, 28, 29] can deal with part of those problems, but still needs improvements to cope with free-floating and spherical joints for humans and humanoids, and to reduce computational cost as well.

Concerning control issues, the optimization technique can be used to build a controller to achieve the generated trajectory. Recently, control frameworks based on quadratic programming (QP) for digital humans and humanoid including multiple contacts with the environments [17, 31, 7, 32, 8], extending the model predictive control (MCP) applied to simplified model of bipedal locomotion [13, 34]. The basic approach is to compute the control input to reduce the errors between the desired tasks and their current state from sensors, anticipating the future for a finite horizon. For those controllers to be applied to full whole-body model in real-time motion generation, efficient analytical gradient computation is a critical issue as well.

In this paper, we present a new framework of trajectory optimization and its applications for anthropomorphic systems based on a comprehensive differential kinematics and dynamics [5, 6]. After introducing the comprehensive motion transformation matrix (CMTM), we show some useful formulae allowing computation of Jacobians of physical quantities with respect to joint angles and its derivatives. Examples of optimization for redundant manipulator with spherical joints and PE trajectory for a humanoid are demonstrated to validate the effectiveness of the proposed framework. Especially, the analytical gradient of zero moment point (ZMP) [33] with respect to joint angles and their derivatives has never been shown and used for dynamic humanoid motion optimization in previous work. Utilization of the framework for optimal control is then discussed before concluding the paper.

2 New Optimization Framework using CMTM

This chapter outlines the new optimization framework using CMTM [5]. We will briefly introduce its definition and derivation of useful analytical Jacobians for various physical quantities with respect to joint angles and its derivatives.

2.1 Optimization formulation

Here the trajectories of the generalized coordinates of a robot $\boldsymbol{q}$ are parameterized by a vector $\boldsymbol{a}$ and time instance t, namely $\boldsymbol{q}(\boldsymbol{a},t)$. This parameterization can be for instance Fourier series, polynomial interpolation, or B-splines, which allows computation of their derivatives $\dot{\boldsymbol{q}}$ and $\ddot{\boldsymbol{q}}$ with respect to $\boldsymbol{a}$ and t depending on the implemented trajectory parameterization.

By defining a vector $\boldsymbol{Q} = [\boldsymbol{q}^T \dot{\boldsymbol{q}}^T \ddot{\boldsymbol{q}}^T]^T$, physical quantities $\boldsymbol{y}$ are expressed by using $\boldsymbol{Q}$, such as the position, orientation, linear / angular velocity and acceleration of each link coordinate, the joint torques and the constraint forces acting on the joint coordinates. By combining those quantities we can compute the center of mass (CoM) and their derivatives, or the ZMP that is a point where the horizontal components of moments from the ground reaction force are zero. For j-th time instance t_j, let $\boldsymbol{Q}_j$ denote the coordinates together with their derivatives and $\boldsymbol{y}_{i,j}$ the i-th physi-

cal quantity at t_j, where $\boldsymbol{y}_{i,j}$ constituting $\boldsymbol{Y}$, the whole set of the evaluated quantities. Based on this notation, the trajectory optimization problem can be formulated:

$$\begin{aligned} &\min_{\boldsymbol{a}} \ c(\boldsymbol{Y}) \\ &\text{subject to } \ \forall\, k \ \ g_k(\boldsymbol{Y}) \leq 0 \end{aligned} \tag{1}$$

where c is the cost function to be evaluated and g_k is k-th inequality constraint. Equality constraints are omitted as they can be represented by two inequalities.

The optimization needs the gradient of the cost function and the constraints, which is computationally expensive if we compute it numerically. The following analytical gradient computation is therefore necessary for efficient optimization:

$$\frac{\partial h}{\partial \boldsymbol{a}} = \sum_i \sum_j \frac{\partial h}{\partial \boldsymbol{y}_{i,j}} \frac{\partial \boldsymbol{y}_{i,j}}{\partial \boldsymbol{Q}_j} \frac{\partial \boldsymbol{Q}_j}{\partial \boldsymbol{a}} \ \ (h = c \ \ or \ \ g_k) \tag{2}$$

The gradient $\partial h/\partial \boldsymbol{y}_{i,j}$ is derived according to the physical quantities involved in the cost function or the constraints, and the partial derivative $\partial \boldsymbol{Q}_j/\partial \boldsymbol{a}$ can be computed from the implemented trajectory parameterization. The term $\partial \boldsymbol{y}_{i,j}/\partial \boldsymbol{Q}_j$ is the partial derivative of physical quantities of multi-body system with respect to the joint coordinates and their derivatives. Its typical example is the basic Jacobian [15], which is the partial derivative of the position and orientation of each link with respect to the joint coordinates. In general, the derivatives of the velocities, the accelerations and the joint torques with respect to $\boldsymbol{q}$, $\dot{\boldsymbol{q}}$, $\ddot{\boldsymbol{q}}$ are required in order to compute $\partial \boldsymbol{y}_{i,j}/\partial \boldsymbol{Q}_j$.

Although previous work [24, 28] formulate the analytical partial derivative of Cartesian coordinates, their derivative, and joint torques with respect to the joint coordinates and their derivatives, it should be extended for spherical joints, free-floating base or other types of joints in order to be applied to anthropomorphic systems, because the formulations are originally designed for fixed manipulators. The computation complexity should also be improved for the partial derivative of the variables of a link using recursive formula, as it is almost O (N_J^2), where N_J is the number of DOF.

2.2 Comprehensive motion transformation matrix (CMTM)

Before introducing the new framework, we provide definitions of variables and notations. The position and orientation matrix of the coordinate system of a rigid body are $\boldsymbol{p}$ and $\boldsymbol{R}$ respectively. Let $\boldsymbol{\omega}$ and $\boldsymbol{v}$ be the linear and angular velocity represented by the local coordinate respectively, then the following relationship holds.

$$\dot{\boldsymbol{R}} = \boldsymbol{R}[\boldsymbol{\omega}\times] \tag{3}$$

$$\boldsymbol{v} = \boldsymbol{R}^T \dot{\boldsymbol{p}} \tag{4}$$

where skew operator is represented as follows:

$$[\boldsymbol{x}\times] \triangleq \begin{bmatrix} 0 & -x_{(3)} & x_{(2)} \\ x_{(3)} & 0 & -x_{(1)} \\ -x_{(2)} & x_{(1)} & 0 \end{bmatrix} \tag{5}$$

The 6×6 transformation matrix of position $\boldsymbol{p}$ and orientation $\boldsymbol{R}$ is defined as follows:

$$\boldsymbol{A}(\boldsymbol{p},\boldsymbol{R}) \triangleq \begin{bmatrix} \boldsymbol{R} & [\boldsymbol{p}\times]\boldsymbol{R} \\ \boldsymbol{O}_3 & \boldsymbol{R} \end{bmatrix} \tag{6}$$

where $\boldsymbol{O}_n$ and $\boldsymbol{E}_n$ are $n\times n$ zero and identity matrices respectively. Linear and angular velocities are concatenated and defined as the following vector:

$$\boldsymbol{v} \triangleq \begin{bmatrix} \boldsymbol{v}^T & \boldsymbol{\omega}^T \end{bmatrix}^T \tag{7}$$

Here, we introduce the operator for linear and angular velocities as follows:

$$[\boldsymbol{v}_{\bullet}] \triangleq \begin{bmatrix} [\boldsymbol{\omega}\times] & [\boldsymbol{v}\times] \\ \boldsymbol{O}_3 & [\boldsymbol{\omega}\times] \end{bmatrix}, \quad \boldsymbol{v}_1 \bullet \boldsymbol{v}_2 \triangleq [\boldsymbol{v}_{1\bullet}]\boldsymbol{v}_2 \tag{8}$$

This operator satisfies several important axioms like bilinearity, alternativity, and Jacobi identity. For the sake of explanation, we utilize variation $\delta\boldsymbol{\alpha}$ instead of $\boldsymbol{v}$ in the following formulations. The variation of $\boldsymbol{A}$ can be written as:

$$\delta\boldsymbol{A} = \boldsymbol{A}[(\delta\boldsymbol{\alpha})_{\bullet}] \tag{9}$$

Let us now define the following new 18×18 'comprehensive motion transformation matrix (CMTM)" $\boldsymbol{X}$ as follows:

$$\boldsymbol{X}(\boldsymbol{A},\boldsymbol{v},\dot{\boldsymbol{v}}) \triangleq \begin{bmatrix} \boldsymbol{A} & \boldsymbol{O}_6 & \boldsymbol{O}_6 \\ \boldsymbol{A}[\boldsymbol{v}_{\bullet}] & \boldsymbol{A} & \boldsymbol{O}_6 \\ \frac{1}{2}\boldsymbol{A}\left([\dot{\boldsymbol{v}}_{\bullet}]+[\boldsymbol{v}_{\bullet}]^2\right) & \boldsymbol{A}[\boldsymbol{v}_{\bullet}] & \boldsymbol{A} \end{bmatrix} \tag{10}$$

We here define the following variation of 18 dimensional vector:

$$\delta\boldsymbol{x} \triangleq \begin{bmatrix} \delta\boldsymbol{\alpha}^T & \delta\boldsymbol{v}^T & \delta\dot{\boldsymbol{v}}^T \end{bmatrix}^T \tag{11}$$

Vector $\delta\boldsymbol{x}$ is the concatenated vector of the variation of standard 6 dimensional coordinates, velocities, and accelerations. Although $\delta\boldsymbol{x}$ is usually utilized in the standard formulations of differential kinematics, the differential operation of CMTM $\boldsymbol{X}$ will be discussed by newly defining the variation of 18 dimensional vector:

$$\delta\boldsymbol{\xi} \triangleq \begin{bmatrix} \delta\boldsymbol{\alpha}^T & \delta\boldsymbol{\zeta}^T & \delta\boldsymbol{\eta}^T \end{bmatrix}^T \triangleq \boldsymbol{S}\delta\boldsymbol{x} \tag{12}$$

where,

$$\boldsymbol{S}(\boldsymbol{v},\dot{\boldsymbol{v}}) \triangleq \begin{bmatrix} \boldsymbol{E}_6 & \boldsymbol{O}_6 & \boldsymbol{O}_6 \\ -[\boldsymbol{v}_{\bullet}] & \boldsymbol{E}_6 & \boldsymbol{O}_6 \\ -\frac{1}{2}\left([\dot{\boldsymbol{v}}_{\bullet}]-[\boldsymbol{v}_{\bullet}]^2\right) & -\frac{1}{2}[\boldsymbol{v}_{\bullet}] & \frac{1}{2}\boldsymbol{E}_6 \end{bmatrix} \tag{13}$$

Matrix $\boldsymbol{S}$ transforms variation $\delta\boldsymbol{x}$ into that of new vector $\delta\boldsymbol{\xi}$, and note that the inverse matrix of $\boldsymbol{S}$ always exists.

Let us also define the following new matrix and operator:

$$[\delta\boldsymbol{\xi}^{\bullet}] \triangleq \begin{bmatrix} [\delta\boldsymbol{\alpha}.] & \boldsymbol{O}_6 & \boldsymbol{O}_6 \\ [\delta\boldsymbol{\zeta}.] & [\delta\boldsymbol{\alpha}.] & \boldsymbol{O}_6 \\ [\delta\boldsymbol{\eta}.] & [\delta\boldsymbol{\zeta}.] & [\delta\boldsymbol{\alpha}.] \end{bmatrix}, \quad \delta\boldsymbol{\xi}_1{}^{\bullet}\delta\boldsymbol{\xi}_2 \triangleq [\delta\boldsymbol{\xi}_1{}^{\bullet}]\delta\boldsymbol{\xi}_2 \tag{14}$$

Operator $[^{\bullet}]$ also shows the similar features as operator $[\times]$ and $[.]$ in **Eq.**(5) and **Eq.**(8). By introducing the new vector and operator, the variation of $\boldsymbol{X}$ can be written in the similar form as **Eq.**(9), and we can have:

$$\delta\boldsymbol{X} = \boldsymbol{X}[(\delta\boldsymbol{\xi})^{\bullet}] \tag{15}$$

The similarity between **Eq.**(9) and **Eq.**(15) plays an important role when introducing the Jacobians of physical quantities with respect to joint angles and its derivatives, which is detailed in [5].

Concerning the robot dynamics, inertial properties of a rigid body consist of mass m, CoM $\boldsymbol{c}$, and inertia tensor $\boldsymbol{I}_c$. They can be summarized as the following 6×6 matrix:

$$\boldsymbol{M} \triangleq \begin{bmatrix} m\boldsymbol{E}_3 & m[\boldsymbol{c}\times]^T \\ m[\boldsymbol{c}\times] & \boldsymbol{I}_c + m[\boldsymbol{c}\times][\boldsymbol{c}\times]^T \end{bmatrix} \tag{16}$$

Defining the inertial forces of a rigid body $\widehat{\boldsymbol{f}}$ and the moment around its coordinate $\boldsymbol{n}$ represented in global frame, let us define 6-axis force $\boldsymbol{f}$ represented by the local coordinate as follows:

$$\boldsymbol{f} \triangleq \left[\boldsymbol{R}\widehat{\boldsymbol{f}}^T \ \boldsymbol{R}\boldsymbol{n}^T\right]^T \tag{17}$$

The equations of motion of a rigid body, and its variation can be written as:

$$\boldsymbol{f} = \boldsymbol{M}\dot{\boldsymbol{v}} - [\boldsymbol{v}.]^T\boldsymbol{M}\boldsymbol{v} \tag{18}$$

$$\delta\boldsymbol{f} = \boldsymbol{M}\delta\dot{\boldsymbol{v}} - \boldsymbol{D}\delta\boldsymbol{v} \ = \ \boldsymbol{H}\delta\boldsymbol{x} \tag{19}$$

$$\boldsymbol{H} \triangleq \left[\boldsymbol{O}_6 \ \boldsymbol{D} \ \boldsymbol{M}\right] \tag{20}$$

by introducing a matrix $\boldsymbol{D}$ [5].

Here we also define the variables of kinematic chain: $\boldsymbol{q}_i$ is n_{Ji} set of joint variables (angles) where n_{Ji} is the number of DOF of joint i; in the same way, $\boldsymbol{\psi}_i$ denotes the joint velocity variables. We can define the following variation of $3n_{Ji}$ dimensional vector consisting of the variations of joint variable, velocity, and its derivative:

$$\delta\boldsymbol{\chi} \triangleq \left[\delta\boldsymbol{q}^T \ \delta\boldsymbol{\psi}^T \ \delta\dot{\boldsymbol{\psi}}^T\right]^T \tag{21}$$

and the relationship between $\delta\boldsymbol{x}_i^{p(i)}$ and $\delta\boldsymbol{\chi}_i$ is summarized as follows [5]:

$$\delta \boldsymbol{x}_i^{p(i)} = \boldsymbol{G}_i \delta \boldsymbol{\chi}_i = \left[\boldsymbol{K}_i{}^T \delta \boldsymbol{q}^T \ \boldsymbol{K}_i{}^T \delta \boldsymbol{\psi}^T \ \boldsymbol{K}_i{}^T \delta \dot{\boldsymbol{\psi}}^T \right]^T \tag{22}$$

where $p(i)$ and $\boldsymbol{K}_i$ are the index of a root-side link connected to link i, and $6 \times n_{Ji}$ constant selection matrix specifying the axes of the DOF of the joint i respectively. For example, if joint i_1 has z-axis rotational joint and joint i_2 has a spherical joint, the corresponding matrices are followings:

$$\boldsymbol{K}_{i_1} = \left[0\ 0\ 0\ 0\ 0\ 1 \right]^T, \ \boldsymbol{K}_{i_2} = \left[\boldsymbol{O}_3 \ \boldsymbol{E}_3 \right]^T \tag{23}$$

2.3 Analysis on Arbitrary Jacobian

As a result of differential analysis [5], we can derive the following differential relationship between the variation $\delta \boldsymbol{\xi}_j$ of link j and those of root-side links $\delta \boldsymbol{\xi}_k^{p(k)}$ as follows:

$$\delta \boldsymbol{\xi}_j = \sum_{k \in \mathscr{P}(j)} \boldsymbol{X}_k^j \, \delta \boldsymbol{\xi}_k^{p(k)} \tag{24}$$

where $\mathscr{P}(i)$ is the set of all root-side links recursively connected to link i, including i, and $\boldsymbol{X}_k^j$ denotes the relative matrix $\boldsymbol{X}$ of link j with respect to k. The coefficient matrix of **Eq.**(24) means the Jacobian matrix with respect to $\delta \boldsymbol{\xi}$, and each block matrix is equal to relative CMTM $\boldsymbol{X}_k^{p(k)}$.

By utilizing **Eq.**(12), the following equation is obtained.

$$\delta \boldsymbol{x}_j = \sum_{k \in \mathscr{P}(j)} \boldsymbol{S}_j{}^{-1} \boldsymbol{X}_k^j \boldsymbol{S}_k^{p(k)} \delta \boldsymbol{x}_k^{p(k)} = \sum_{k \in \mathscr{P}(j)} \widehat{\boldsymbol{X}}_k^j \delta \boldsymbol{x}_k^{p(k)} \tag{25}$$

The next transformation can be performed with **Eq.**(22) as follows:

$$\delta \boldsymbol{x}_j = \sum_k \boldsymbol{J}_{(j,k)} \delta \boldsymbol{\chi}_k^{p(k)} \tag{26}$$

$$\boldsymbol{J}_{(j,k)} \triangleq s_{(j,k)} \widehat{\boldsymbol{X}}_k^j \boldsymbol{G}_k \tag{27}$$

where, $s_{(j,k)}$ is equal to 1 when $k \in \mathscr{P}(j)$, and otherwise is equal to 0.

This is analogous to the basic Jacobian [15] as shown in the **Fig.**1:

$$\delta \boldsymbol{\alpha}_j = \sum_{k \in \mathscr{P}(j)} \boldsymbol{A}_k^j \delta \boldsymbol{\alpha}_k^{p(k)} \tag{28}$$

The Jacobian of link internal forces can also be derived as follows:

$$\delta \boldsymbol{f}_j = \boldsymbol{L}_j \delta \boldsymbol{\chi}_{\text{all}} = \sum_k \boldsymbol{L}_{(j,k)} \delta \boldsymbol{\chi}_k \tag{29}$$

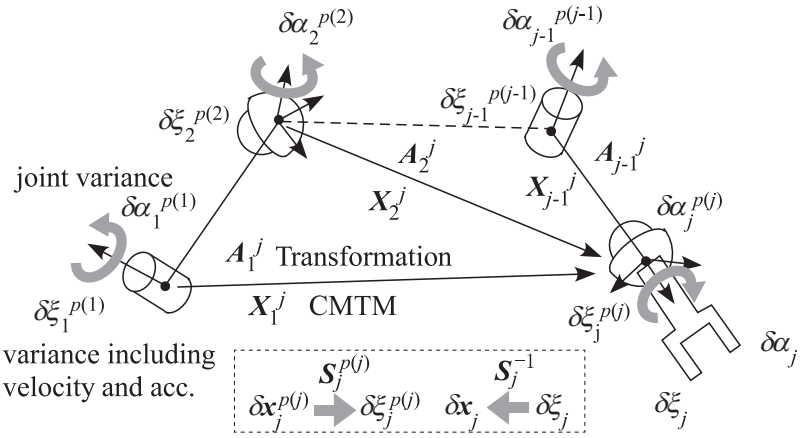

Fig. 1 The relationship between basic Jacobian and the variance defined with CMTM. The new framework can also be applied to free-floating and spherical joints.

where

$$\boldsymbol{L}_{(j,k)} = \boldsymbol{H}_j \boldsymbol{J}_{(j,k)} \tag{30}$$

In the same way, the variation of the joint constraint force $\boldsymbol{f}_j^{p(j)}$ of link j can be computed as:

$$\delta \boldsymbol{f}_j^{p(j)} = \boldsymbol{N}_j \delta \boldsymbol{\chi}_{\text{all}} = \sum_k \boldsymbol{N}_{(j,k)} \delta \boldsymbol{\chi}_k \tag{31}$$

where

$$\boldsymbol{N}_{(j,k)} = \begin{cases} \widehat{\boldsymbol{H}}_j \boldsymbol{J}_{(j,k)} & (k \in \mathscr{P}(j)) \\ \boldsymbol{A}_k^{j-T} \left(\widehat{\boldsymbol{H}}_k \boldsymbol{J}_{(k,k)} - [\boldsymbol{f}_k^{p(k)} \hat{\cdot}] \boldsymbol{T} \boldsymbol{G}_k \right) & (k \in \mathscr{C}(j)) \\ \boldsymbol{O}_{6\times 18} & (others) \end{cases} \tag{32}$$

$$\widehat{\boldsymbol{H}}_j = \boldsymbol{H}_j + \sum_{k \in C(j)} \boldsymbol{A}_k^{j-T} \widehat{\boldsymbol{H}}_k \boldsymbol{S}_k{}^{-1} \boldsymbol{X}_j^k \boldsymbol{S}_j \tag{33}$$

$$\boldsymbol{T} \triangleq [\boldsymbol{E}_6 \;\; \boldsymbol{O}_6 \;\; \boldsymbol{O}_6] \tag{34}$$

$$\text{operation } [\hat{\cdot}] \triangleq \begin{bmatrix} \boldsymbol{O}_3 & \left[\widehat{\boldsymbol{f}}\times\right] \\ \left[\widehat{\boldsymbol{f}}\times\right] & [\boldsymbol{n}\times] \end{bmatrix}, \;\; [\widehat{\boldsymbol{f}}_1 \cdot]^T \widehat{\boldsymbol{f}}_2 = [\widehat{\boldsymbol{f}}_2 \hat{\cdot}] \widehat{\boldsymbol{f}}_1 \tag{35}$$

where $C(k)$ is the set of leaves-side links connected to link k, and $\mathscr{C}(k)$ is the set of all leaves-side links recursively connected to link k.

Before computing Jacobian $\boldsymbol{N}_{(j,k)}$, matrix $\widehat{\boldsymbol{H}}_j$ for all the links needs to be computed in advance according to recursive formula **Eq.**(33). After updating $\widehat{\boldsymbol{H}}_j$ for all

links, matrix $\boldsymbol{N}_{(j,k)}$ for any j and k can be directly computed by **Eq.**(32). Those computation can be performed with the computational cost $O(N_J)$ [5].

3 Applications

This section presents examples of application of the proposed framework, first optimization of dynamic collision-free motion of redundant robot arm composed of spherical joints and next whole-body PE trajectory for dynamic parameter identification of a humanoid robot [6].

3.1 Dynamic collision-free motion for redundant robot

We applied the proposed optimization framework to a redundant serial robot manipulator composed of five spherical joints in a complex environment cluttered

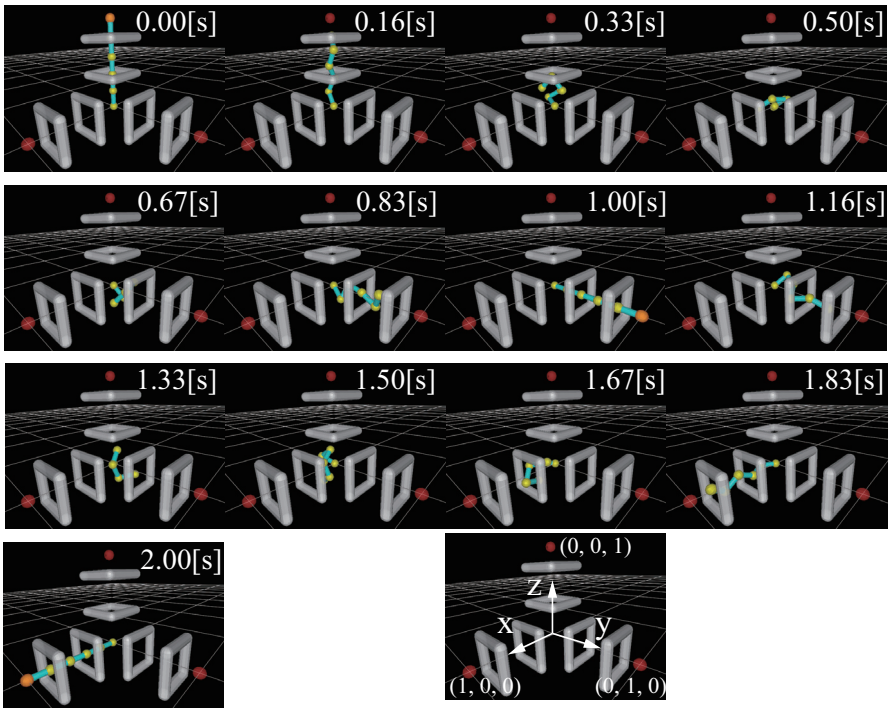

Fig. 2 Snapshots of the generated motion of the redundant robot in a cluttered environment. Starting from the initial position [0 0 1], the target end-effector positions (bottom-right) at [0 1 0] and [1 0 0] were achieved without collision to obstacles (video in the supplementary material).

with non-convex obstacles and no gravity. Each link has the identical physical properties: for link i, $\boldsymbol{p}_i^{p(i)} = [0\ 0\ 0.2]$ [m], $m_i = 3.0$ [kg], $\boldsymbol{c}_i = [0\ 0\ 0.1]$ [kgm], $\boldsymbol{I}_{ci} = \mathrm{diag}([11.2\ 11.2\ 2.4]) * 10^{-3}$ [kgm^2] with its base spherical joint is fixed at $[0\ 0\ 0]$. As shown on the bottom-right in **Fig.**2, starting from $\boldsymbol{p}_e^0 = [0\ 0\ 1]$ at $t = 0.0$, the end-effector of the manipulator should pass through the points $\boldsymbol{p}_e^1 = [0\ 1\ 0]$ at $t = 1.0$ [s], before stopping at $\boldsymbol{p}_e^2 = [1\ 0\ 0]$ at $t = 2.0$ [s] with zero joint velocities and accelerations. Six square-shape hollow obstacles composed of four cylinders whose diameter and length are 0.1 [m] and 0.4 [m] are placed such that their center is at the distance of 0.4 and 0.8 from the origin along each of x, y and z axes.

The trajectory of spherical joints is parameterized by using B-splines as in [29], expressing their joint angles with an angle-axis vector. During the movement, the joint torque limitations are considered; $|\tau_{1,k}| < 0.1$ [Nm] and $|\tau_{j,k}| < 20.0$ [N] $(2 \leq j \leq 5)$, which means the torque of the base spherical joint is limited to a very low value. In order to avoid collisions and self-collisions, constraints on the distance from joint k to the closest obstacle d_k and to the link l should also be satisfied; $d_k \geq 0.15$ and $||\boldsymbol{p}_k - \boldsymbol{p}_l|| \geq 0.1 (k \neq l)$ so that a sphere of diameter 0.1[m] around the joint does not collide.

All the constraint conditions were taken into account according to penalty function method. The optimization itself was solved by quasi-Newton method [10] by utilizing the proposed framework. As shown in **Fig.**2, the end-effector successfully passed through the targeted positions without colliding obstacles. As can be seen in **Fig.**3 showing the resultant joint torque of the base spherical joint, the torque of all the axes satisfy the desired limitations, which has been difficult with conventional optimization methods.

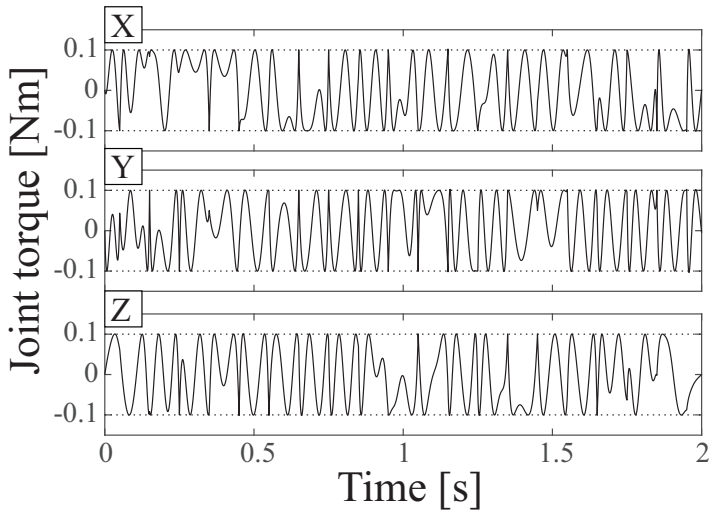

Fig. 3 Resultant joint torque trajectories of the base spherical joint. The torque limit of small value of $\pm 0.1[Nm]$ is satisfied throughout the motion.

3.2 Optimization of humanoid PE trajectory for identification

In order to optimize the PE trajectory for dynamic parameter identification of a humanoid robot, the condition number of the "regressor matrix" obtained from joint trajectory should be minimized while maintaining dynamic constraints. Although we showed an analytical framework to optimize the condition number in our previous work [3], the stability was considered only statically by using the CoM, which is conservative and may limit the identification performance. In the resultant motions, both feet were placed to the ground as the dynamic stability condition becomes too severe to be satisfied only by the CoM condition. This limitation makes it difficult to generate dynamic leg motions by standing on one leg for better identification.

To solve this issue, we here derive analytical computation of Jacobian of the ZMP based on the proposed framework to use it as the dynamic stability constraint in the trajectory optimization. The joint torque $\boldsymbol{\tau}_j$, a n_{Ji} dimensional vector, can be obtained as:

$$\boldsymbol{\tau}_j = \boldsymbol{K}_j{}^T \boldsymbol{f}_j^{p(j)} \tag{36}$$

Its variance can be be extracted from the corresponding component of $\boldsymbol{N}_{(j,i)}$ as follows:

$$\delta\boldsymbol{\tau}_j = \widehat{\boldsymbol{N}}_j \delta\boldsymbol{\chi}_{\text{all}} = \sum_i \widehat{\boldsymbol{N}}_{(j,i)} \delta\boldsymbol{\chi}_i \tag{37}$$

$$\widehat{\boldsymbol{N}}_{(j,i)} \triangleq \boldsymbol{K}_j{}^T \boldsymbol{N}_{(j,i)} \tag{38}$$

The total external forces acting on the kinematic chain are equivalent to $\boldsymbol{f}_W^{p(W)}$ where index W means the world coordinate is connected to floating base link 0. By redefining $\boldsymbol{F}_{ex} \triangleq \boldsymbol{f}_w^{p(w)}$, we can obtain ZMP of $\boldsymbol{F}_{ex}$ projected, for example, on x-y plane.

$$\boldsymbol{F}_{ex} \triangleq \begin{bmatrix} F_{ex(1)} & \cdots & F_{ex(6)} \end{bmatrix}^T \tag{39}$$

$$\boldsymbol{p}_{ZMP} \triangleq \begin{bmatrix} -F_{ex(5)}/F_{ex(3)} & F_{ex(4)}/F_{ex(3)} & 0 \end{bmatrix}^T \tag{40}$$

Jacobian matrix of $\boldsymbol{p}_{ZMP}$ can therefore be easily computed by utilizing $\boldsymbol{N}_{(W,i)}$ as follows:

$$\delta\boldsymbol{p}_{ZMP} = \sum_i \left(\boldsymbol{Z}\boldsymbol{N}_{(W,i)}\right) \delta\boldsymbol{\chi}_i \tag{41}$$

$$\boldsymbol{Z} \triangleq \begin{bmatrix} 0 & 0 & \frac{F_{ex(5)}}{F_{ex(3)}{}^2} & 0 & -\frac{1}{F_{ex(3)}} & 0 \\ 0 & 0 & -\frac{F_{ex(4)}}{F_{ex(3)}{}^2} & \frac{1}{F_{ex(3)}} & 0 & 0 \\ 0 & 0 & 0 & 0 & 0 & 0 \end{bmatrix} \tag{42}$$

We have derived a dynamically stable optimal PE trajectory on one leg by constraining the ZMP inside the area of 4 [cm] and 1 [cm] around the center of the

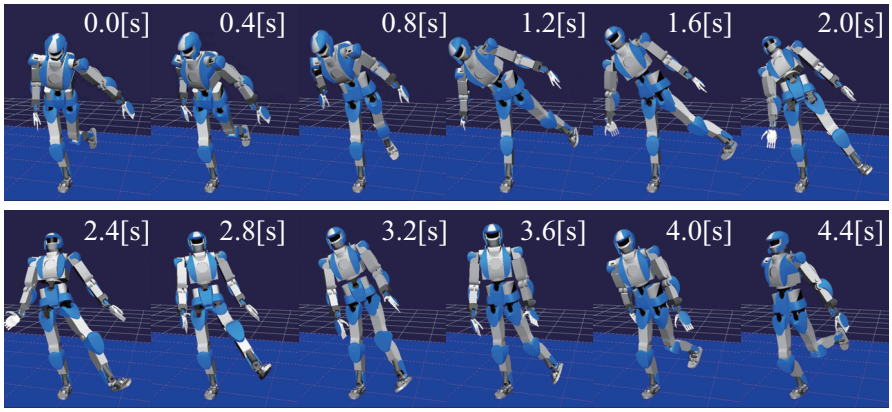

Fig. 4 Snapshots of optimized one-leg PE trajectory for dynamic parameter identification. The humanoid robot HRP-4 can successfully perform resultant whole-body motion by also exciting the free leg (video in the supplemental material).

standing foot in front and lateral direction. The trajectory is parameterized by B-Spline by using physical properties from the robot CAD model. We also added constraints on forces and torque applied on the ankle so that the horizontal forces $F_{ex(1)}, F_{ex(2)}$ and torque $F_{ex(6)}$ stay within $\pm$20[N], $\pm$20[N], $\pm$4[Nm] respectively to avoid slipping. As shown in snapshots in **Fig.**4, the humanoid HRP-4 [14] successfully performed the optimized PE trajectory on dynamic simulator Choreonoid [22], which validates the feasibility. Note that this one-leg dynamic motion cannot be generated with the previous method [3] considering only CoM for stability.

4 Discussions: Controller based on Proposed Framework

The formulation using CMTM can potentially extend the arguments on conventional generic trajectory tracking control in such a way that they include velocity and acceleration. We believe that various Jacobians derived by CMTM can be applied to whole-body cooperative control currently using the basic Jacobian in future developments. The proposed framework of trajectory optimization has high affinity to Model Predictive Control (MPC) or Receding Horizon Control that determines control input for a finite horizon. It optimizes the integrated evaluation function of the state variables or control inputs on the finite horizon, based on discrete equations describing system equation and its time integral.

MPC has been applied to walking motion control for humanoid robots by researchers as Kajita and Wieber [13, 34, 8]. By approximating the whole-body dynamics as a concentrated mass model, those studies have been investigating a linear system equation whose state variables are the CoM position, velocity and acceleration using the CoM jerk as the system input. Constraints related to ZMP and other

state variables are also taken into account in case of humanoid to guarantee its balance condition. In above studies on locomotion, the input jerk is determined based on the evaluation function to minimize the tracking error of state and the jerk itself.

Just like mapping Cartesian states into joint angles through basic Jacobian as is often the case in position-based tracking control, the state variables on velocity, acceleration and ZMP can also be mapped in the same way by using the proposed framework. Since the jerk is regarded as the variance of acceleration, it may be used as trajectory parameter $\boldsymbol{a}$, or the optimization problem of MPC may be formulated as the evaluation function **Eq.**(1) itself in the presented trajectory optimization framework.

In general, the solution of the evaluation function should satisfy the necessary condition that the gradient of the extended Lagrangian function should be equal to zero. The derivation of analytical gradient therefore plays an important role to determine the control inputs and to investigate the system stability [34]. The most advantageous feature of the proposed comprehensive framework is its capability to analytically formulate the gradient of arbitrary physical quantities with respect to motion trajectory. Having started studying this new framework, we intend to come up with a new theoretical basis on determination of input or stability analysis for various control problems of anthropomorphic systems including humanoids and digital humans.

5 Conclusion

In this paper, we addressed a new framework for trajectory optimization based on comprehensive differential kinematics and dynamics that allows dealing with the gradient of any physical quantities with respect to position and its derivatives in the same way as conventional differential kinematics. We introduced a matrix called CMTM, an extended version of transformation matrix by adding velocity and acceleration, and showed that it has the same property as the transformation matrix to apply the chain rules and Jacobian computations. It was also shown that the gradient of physical quantities such as forces applied to links and joints can be computed analytically. Another advantage is that the proposed method can deal with spherical joint, which is critical to analyze human models.

A couple of application examples were presented to demonstrate the usefulness of the proposed framework. We first showed dynamic trajectory optimization of a redundant serial robot manipulator composed of spherical joints. A collision-free dynamic motion was successfully generated in a cluttered environment with non-convex obstacles, imposing a strong torque limit at the same time. This validates the basic trajectory optimization capacity of the proposed framework under severe constraints. Another application is optimization of PE trajectory for identification of dynamic parameters of a humanoid robot. In this example, analytical gradient of ZMP with respect to joint angle and its derivatives was utilized to guarantee the

balance. Dynamic one-leg PE motions were generated whose validity was confirmed by dynamic simulator.

Finally, we discussed the potential of the proposed framework for building controllers. Combining with MPC, we believe its ability of analytical computation of gradient of any physical quantities with respect to joint trajectory can bring a new perspective to the optimal control of anthropomorphic systems. Especially, MPC is heavily utilized for humanoid walking and whole-body control on a simplified model, we expect to contribute to development of such a controller for full anthropomorphic model. We will also push forward the research to apply the proposed framework to human motion modeling and analysis through efficient and accurate computation.

Acknowledgments

This research has been partly supported by Japan Society for the Promotion of Science (JSPS) Grant-in-Aid for Scientific Research (A) Number 17H00768.

References

1. Ayusawa, K., Morisawa, M., Yoshida, E.: Motion retargeting for humanoid robots based on identification to preserve and reproduce human motion features. In: Proc. 2015 IEEE/RSJ Int. Conf. on Intelligent Robots and Systems, pp. 2774–2779 (2015)
2. Ayusawa, K., Nakamura, Y.: Fast inverse kinematics algorithm for large dof system with decomposed gradient computation based on recursive formulation of equilibrium. In: Proc. IEEE/RSJ Int. Conf. on Intelligent Robots and Systems, pp. 3447–3452 (2012)
3. Ayusawa, K., Rioux, A., Yoshida, E., Venture, G., Gautier, M.: Generating persistently exciting trajectory based on condition number optimization. In: Proc. 2017 IEEE Int Conf. Robotics and Automation, pp. 6518–6524 (2017)
4. Ayusawa, K., Venture, G., Nakamura, Y.: Identification of humanoid robots dynamics using floating-base motion dynamics. In: Proc. 2008 IEEE/RSJ Int. Conf. on Intelligent Robots and Systems, pp. 2854–2859 (2008)
5. Ayusawa, K., Yoshida, E.: Comprehensive theory of differential kinematics and dynamics for motion optimization. In: Robotics: Science and Systems XIII (2017)
6. Ayusawa, K., Yoshida, E.: Comprehensive theory of differential kinematics and dynamics towards extensive motion optimization framework. Int. J. Rob. Res. (2018). Under review
7. Bouyarmane, K., Kheddar, A.: On the dynamics modeling of free-floating-base articulated mechanisms and applications to humanoid whole-body dynamics and control. In: Proc. 2012 IEEE-RAS Int. Conf. on Humanoid Robots, pp. 36–42 (2012)
8. Caron, S., Kheddar, A.: Multi-contact walking pattern generation based on model preview control of 3D com accelerations. In: Proc. 2016 IEEE-RAS Int. Conf. on Humanoid Robots, pp. 550–557 (2016)
9. Dai, H., Valenzuela, A., Tedrake, R.: Whole-body motion planning with centroidal dynamics and full kinematics. In: Proc. 2014 IEEE-RAS Int. Conf. on Humanoid Robots, pp. 295–302 (2014)
10. Fletcher, R.: Practical Methods of Optimization; (2Nd Ed.). Wiley-Interscience (1897)

11. Imamura, Y., Ayusawa, K., Yoshida, E.: Risk estimation for intervertebral disc pressure through musculoskeletal joint reaction force simulation. In: Proc. 39th IEEE Annual Int. Conf. Engineering in Medicine and Biology Society (2017). To appear
12. Jovic, J., Escande, A., Ayusawa, K., Yoshida, E., Kheddar, A., Venture, G.: Humanoid and human inertia parameter identification using hierarchical optimization. IEEE Transaction on Robotics **32**(3), 726–735 (2016). DOI 10.1109/TRO.2016.2558190
13. Kajita, S., Kanehiro, F., Kaneko, K., Fujiwara, K., Harada, K., Yokoi, K., Hirukawa, H.: Biped walking pattern generation by using preview control of zero-moment point. In: Proc. 2003 IEEE Int. Conf. on Robotics and Automation, pp. 1620–1626 (2003)
14. Kaneko, K., Kanehiro, F., Morisawa, M., Akachi, K., Miyamori, G., Hayashi, A., Kanehira, N.: Humanoid robot HRP-4 - humanoid robotics platform with lightweight and slim body. In: Proc. 2011 IEEE/RSJ Int. Conf. on Intelligent Robots and Systems, pp. 4400–4407 (2011)
15. Khatib, O.: A unified approach for motion and force control of robot manipulators: The operational space formulation. International Journal of Robotics Research **3**(1), 43–53 (1987)
16. Lengagne, S., Vaillant, J., Yoshida, E., Kheddar, A.: Generation of whole-body optimal dynamic multi-contact motions. International Journal of Robotics Research **32**(9-10), 11041119 (2013). DOI 10.1177/0278364913478990
17. Liu, M., Micaelli, A., Evrard, P., Escande, A., Andriot, C.: Interactive virtual humans: A two-level prioritized control framework with wrench bounds. IEEE Trans. on Robotics **28**(6), 1309–1322 (2012)
18. Miossec, S., Yokoi, K., Kheddar, A.: Development of a software for motion optimization of robots - application to the kick motion of the hrp-2 robot. In: Proc. 2006 IEEE Int. Conf. on Robotics and Biomimetics, pp. 299–304 (2006)
19. Mombaur, K.: Using optimization to create self-stable human-like running. Robotica **27**, 321–330 (2009)
20. Murai, A., Kurosaki, K., Yamane, K., Nakamura, Y.: Computationally fast estimation of muscle tension for realtime bio-feedback. In: Proc. 31st Annual International Conference of the IEEE EMBS, pp. 6546–6549 (2009)
21. Nakamura, Y., Yamane, K., Fujita, Y., Suzuki, I.: Somatosensory computation for man-machine interface from motion-capture data and musculoskeletal human model. IEEE Trans. on Robotics **21**(1), 58–66 (2005)
22. Nakaoka, S.: Choreonoid: Extensible virtual robot environment built on an integrated gui framework. In: Proc. 2012 IEEE/SICE International Symposium on System Integration, pp. 79–85 (2012)
23. Nakaoka, S., Komura, T.: Interaction mesh based motion adaptation for biped humanoid robots. In: Proc. 2012 IEEE-RAS Int. Conf. on Humanoid Robots, pp. 625–631 (2012)
24. Park, F.C., Bobrow, J.E., Ploen, S.R.: A lie group formulation of robot dynamics. Int. J. of Robotics Research **14**(6), 609–618 (1995)
25. Ramirez-Alpizar, I.G., Harada, K., Yoshida, E.: Motion planning for dual-arm assembly of ring-shaped elastic objects. In: Proc. 2014 IEEE-RAS Int. Conf. on Humanoid Robots, pp. 594–600 (2014)
26. Ratliff, N., Zucker, M., Bagnell, J.A., Srinivasa, S.: CHOMP: Gradient optimization techniques for efficient motion planning. In: Proc. 2009 IEEE Int. Conf. on Roboics and Automation, pp. 489–494 (2009)
27. Schulman, J., Ho, J., Lee, A., Awwal, I., Bradlow, H., Abbeel, P.: Finding locally optimal, collision-free trajectories with sequential convex optimization. In: Proc. Robotics: Science and Systems IX (2013)
28. Sohl, G.A., Bobrow, J.E.: A recursive multibody dynamics and sensitivity algorithm for branched kinematic chains. J. of Dyn. Sys., Meas., Control **123**(3), 391–399 (2001)
29. Suleiman, W., Yoshida, E., Kanehiro, F., Laumond, J.P., Monin, A.: On human motion imitation by humanoid robot. In: Proc. 2008 IEEE Int Conf. Robotics and Automation, pp. 2697–2704 (2008)
30. Suleiman, W., Yoshida, E., Laumond, J.P., Monin, A.: On humanoid motion optimization. In: Proceedings of 7th IEEE-RAS International Conference on Humanoid Robots, pp. 180–187 (2007)

31. Tassa, Y., Erez, T., Todorov, E.: Synthesis and stabilization of complex behaviors through online trajectory optimization. In: Proc. 2012 IEEE/RSJ Int. Conf. on Intelligent Robots and Systems, pp. 4906–4913 (2012)
32. Vaillant, J., Kheddar, A., Audren, H., Keith, F., Brossette, S., Escande, A., Bouyarman, K., Kaneko, K., Morisawa, M., Gergondet, P., Yoshida, E., Kajita, S., Kanehiro, F.: Multi-contact vertical ladder climbing with an hrp-2 humanoid. Autonomous Robots **40**(3), 561580 (2016). DOI 10.1007/s10514-016-9546-4
33. Vukobratović, M., Borovac, B.: Zero-moment point - thirty-five years of its life. Int. J. Humanoid Robotics **1**(1), 157–174 (2004)
34. Wieber, P.B.: Trajectory free linear model predictive control for stable walking in the presence of strong perturbations. In: Proc. 2006 IEEE-RAS Int. Conf. on Humanoid Robots, pp. 137–142 (2006)
35. Yamane, K., Anderson, S.O., Hodgins, J.K.: Controlling humanoid robots with human motion data: Experimental validation. In: Proc. 2010 IEEE-RAS Int. Conf. on Humanoid Robots, pp. 504–510 (2010)
36. Yoshida, E., Belousov, I., Esteves, C., Laumond, J.P.: Humanoid motion planning for dynamic tasks. In: Proceedings of 5th IEEE-RAS International Conference on Humanoid Robots, pp. 1–6 (2005)
37. Yoshida, E., Esteves, C., Belousov, I., Laumond, J.P., Sakaguchi, T., Yokoi, K.: Planning 3D collision-free dynamic robotic motion through iterative reshaping. IEEE Trans. on Robotics **24**(5), 1186–1198 (2008). DOI 10.1109/TRO.2008.2002312
38. Yoshida, E., Kanoun, O., Esteves, C., Laumond, J.P., Yokoi, K.: Task-driven support polygon reshaping for humanoids. In: Proceedings of 6th IEEE-RAS International Conference on Humanoid Robots, pp. 827–832 (2006)